Smart Materials and Devices
https://doi.org/10.70401/smd.2026.0056

Supplementary information

Carbon black modified engineered cementitious composite-based triboelectric nanogenerator for mechanical energy harvesting and self-powered cathodic protection

Yinghui Wu, Chen Zhang, Jiawei Wu, Menghuan Guo, Xiaoxu Huang, Biao Hu, Qi Luo, Guoxu Liu

Experimental section

1. Raw materials and mix proportion

This study employed 52.5R ordinary Portland cement (OPC) as the primary binder. Limestone powder (LP) was used as a partial replacement for OPC to improve the workability of the mixture. S95 ground granulated blast-furnace slag (GGBFS) was incorporated to enhance matrix toughness and crack resistance, while quartz sand served as the fine aggregate and contributed to the formation of the skeletal framework of the ECC. Polyethylene (PE) fibers, with a length of 18 mm and a diameter of 24 μm, were added to improve the tensile ductility and toughness of the composite. A high-range water-reducing admixture (HRWRA) was used to regulate the water-to-binder ratio and ensure adequate flowability. The chemical compositions of the cementitious materials are presented in **Table S1**. The carbon black (CB) particles had a diameter of 27-40 nm, an apparent density of 0.06-0.11 g/cm³, and an electrical resistivity below 1.5 Ω·m. Based on preliminary tests, the CB content was varied from 0 to 2.5 wt%. CB dosages below 0.5 wt% were insufficient to establish a continuous conductive network, whereas dosages above 2.5 wt% markedly reduced workability and adversely affected the mechanical properties. Polyvinylpyrrolidone K30 (PVP-K30) was used as a dispersant to promote the uniform distribution of CB within the ECC matrix. Silica fume (SF), owing to its ultrafine particle size, was incorporated to densify the matrix and improve the continuity of the conductive network. In addition, the spherical morphology and lubricating effect of SF facilitated fiber dispersion, thereby helping to preserve the high tensile ductility of the ECC. The mixture proportions of the CB-ECC composites are listed in **Table S2**.

Table S1. Chemical constituents of cementitious composites (wt%)

Materials	CaO	SiO_2	Al_2O_3	MgO	SO_3	K_2O	MnO	Fe_2O_3	LOI
OPC	70.91	15.81	3.59	0.63	2.79	0.91	0.04	4.56	0.76
SF	0.71	97.08	0.42	0.19	0.31	1.09	0.02	0.08	0.1
LP	98.68	0.28	0.11	0.74	-	0.03	-	0.11	0.04
GGBFS	46.43	25.29	14.64	8.33	2.54	0.39	0.51	0.57	1.29

Table S2. Mix design of CB-ECC

	W/C	Cement	GGBFS	Sand	SF	LP	CB	PE (vol%)	HRWRA (kg/m^3)	PVP (kg/m^3)
CB0	0.16	1	1.07	0.71	0.21	0.14	0	2	20	0.5
CB1	0.18						0.01		30	
CB2	0.22						0.02		40	
CB2.5	0.24						0.025		45	

2. Specimen preparation

CB and PVP-K30 dispersant were added to a portion of the deionized water. PVP-K30 adsorbed onto the surface of the CB particles, forming a protective layer that inhibited agglomeration. The suspension was magnetically stirred for 30 min to obtain a uniformly dispersed CB solution. Subsequently, cement, GGBFS, silica fume (SF), LP, and quartz sand were added to a 15 L mixing container and dry-mixed at 60 rpm for 2 min. The CB dispersion, the remaining deionized water, and the high-range water-reducing admixture (HRWRA) were then added sequentially. The mixture was stirred at 60 rpm for 4 min, followed by high-speed mixing at 180 rpm for 1 min. PE fibers were gradually introduced into the fresh matrix and mixed at 60 rpm for at least 4 min to promote uniform fiber distribution. The mixture was then subjected to an additional 1 min of high-speed mixing at 180 rpm to ensure the homogeneity of the fresh ECC slurry. The resulting slurry was cast into molds with dimensions of 50 × 50 × 50 mm³ and 40 × 40 × 5 mm³ for compressive strength and triboelectric performance tests, respectively. After casting, the specimens were covered with plastic film to minimize moisture loss and were demolded after 24 h. The demolded specimens were subsequently cured for 28 days in a curing chamber maintained at 23 ± 3 °C and a relative humidity of 95%.

In addition, to accommodate the rigid characteristics of cement-based materials, a “vertical-separated” structure was adopted for the TENG. Polydimethylsiloxane (PDMS) and a curing agent were mixed in a 10:1 mass ratio to form a homogeneous PDMS sol through ultrasonic treatment. The sol was then placed in a vacuum degassing machine to remove internal air bubbles. To ensure smooth demolding, a layer of release agent (silicone oil) was evenly sprayed onto the surface of

the casting mold. The degassed PDMS sol was then evenly poured into the mold and placed in an oven to dry and cure. Furthermore, aluminum foil was used as the electrode to ensure efficient conversion of the triboelectric effect. After connecting the cut PDMS pieces to the electrodes, they were bonded to the acrylic substrate using an adhesive.

3. Test methods

Compressive Strength: The compressive strength of the CB-ECC specimens was evaluated using 50 × 50 × 50 mm³ cubes. Tests were conducted after 3, 7, and 28 days of curing at a constant loading rate of 0.6 MPa/s. At least three replicate specimens were tested at each curing age, and the average value was reported.

Electrochemical Performance Testing: Electrochemical impedance spectroscopy (EIS) was performed using a CHI660E electrochemical workstation (Shanghai Chenhua Instrument Co., Ltd., China) over a frequency range of 0.1 Hz to 1 MHz. The bulk resistance was determined by fitting the high-frequency semicircular response in the Nyquist plot. The electrical conductivity, σ, was subsequently calculated using Equation (1):

$$\sigma = \frac{L}{RA} \tag{1}$$

Here, L is the distance between the electrodes, A is the electrode specimen contact area, and R is the bulk resistance of the specimen. Further analysis of the relationship between the Porter plot and the phase angle as a function of frequency was conducted to characterize the dielectric relaxation and charge transport mechanisms.

Triboelectric property testing: CBECC was used as the positive triboelectric layer, while PDMS served as the negative triboelectric layer. The PDMS layer was prepared by mixing PDMS base and curing agent at a 10:1 mass ratio, followed by degassing and curing. The final thickness of the PDMS layer was approximately 1 mm. The PDMS surface was not patterned or chemically treated; it was used as-cast with a smooth surface. The surface roughness of the PDMS was approximately Ra = 0.52 μm. The water contact angle of the PDMS is approximately 103.1°, as shown in Figure S1.

Periodic contact–separation motion was generated using a LinMot HS01-37 × 166 linear motor. The CBECC specimen was fixed on a stationary acrylic base, and the PDMS layer was mounted

on the moving arm of the linear motor. The open-circuit voltage was measured using a Keithley 6514 electrometer with an input impedance greater than 200 TΩ to minimize the loading effect. The short-circuit current was measured using a low-noise current preamplifier (SR570, Stanford Research Systems). The transferred charge was measured using a charge amplifier. All cables were shielded and grounded to minimize electromagnetic interference. The electrical output signals were recorded using the corresponding electrical measurement instruments under different various loading frequencies (0.5, 1.0, 1.5, and 2.0 Hz). For the frequency-dependent tests, the force was maintained at 10 N. The separation distance between the CBECC and PDMS surfaces was 1cm in the fully separated state. The effective contact area between the CBECC and PDMS layers was 40 mm × 40 mm (1600 mm^2). The power density was obtained by normalizing the power by the effective contact area:

$$P_d = V \times I/A \quad (1)$$

where V is the output voltage, I is the output current and A is the effective contact area, 0.0016 m^2. V and I were measured across a series of external load resistances (R) ranging from 10^3 to 10^9 Ω. In addition, long-term cyclic tests were conducted to assess the operational stability of the CBECC-TENGs, with the output retention and voltage attenuation used as indicators of durability.

Microscopic Characterization: X-ray diffraction (XRD) analysis was performed using a Bruker D8 Advance diffractometer over a scanning range of 5°–70° to investigate the evolution of the hydration products in the CB-ECC composites. The surface morphology and roughness of the CB-ECC specimens were characterized using a three-dimensional optical profilometer (LK-G5000, Keyence, Japan) to evaluate the influence of CB incorporation on interfacial contact and triboelectric charge generation.

Finite element simulation: The COMSOL simulations were performed using the Electrostatics module in COMSOL Multiphysics 6.0. The geometric dimensions of the model were set to match the experimental device: the CBECC layer was 40 mm × 40 mm × 5 mm, the PDMS layer was 40 mm × 40 mm × 1 mm, and the aluminum electrodes were 40 mm × 40 mm × 0.1 mm. The separation distance between the CBECC and PDMS surfaces was varied from 0 mm (full contact) to 1cm (fully separated). The relative dielectric constant of the PDMS is 2.75, which is provided by the COMSOL software database. The surface charge density on the CBECC surface was set to $+0.6 \times 10^{-7}$ C/m^2, and that on the PDMS surface was set to -0.6×10^{-7} C/m^2, based on typical

values reported for cement-based TENGs. The bottom electrode was set as ground, and the top electrode was set as a terminal with a floating potential. The outer boundaries of the air domain were set as zero charge. A stationary solver was used to calculate the electric potential distribution at different separation distances.

Impressed Current Cathodic Protection (ICCP) Testing: The open-circuit potential (OCP), electrochemical impedance spectroscopy (EIS), and Tafel polarization curves were measured in a 3.5 wt% NaCl solution using the aforementioned CHI660E electrochemical workstation. A3 carbon steel rods with a diameter of 10 mm were used as the working electrodes, while an Ag/AgCl electrode served as the reference electrode. Before electrochemical measurements, the working electrodes were immersed in the 3.5 wt% NaCl solution for 1 h to stabilize the electrode potential and establish a steady interfacial condition.

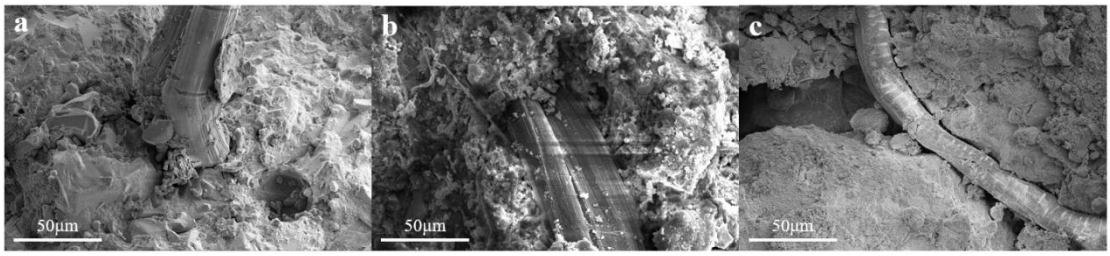


Figure S1. SEM image of CBECC. (a) 0 wt% CB. (b)2.0 wt% CB. (c) 2.5 wt% CB.

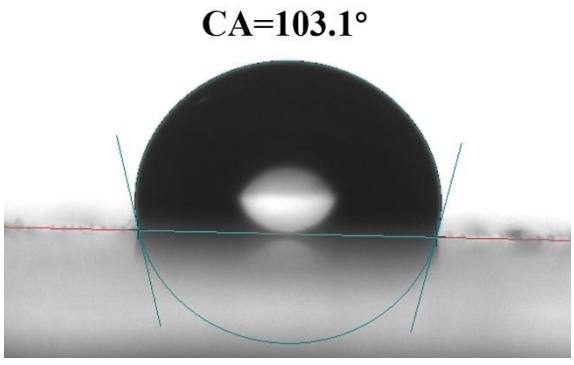


Figure S2. The water contact angle of PDMS.

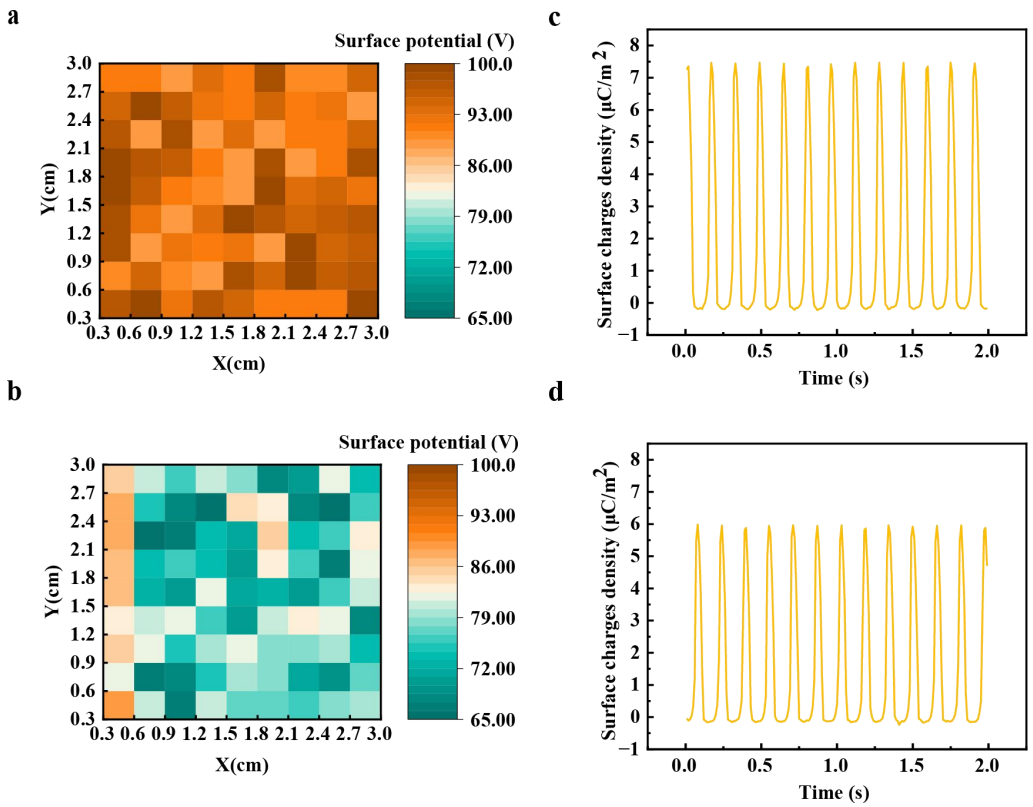


Figure S3. Surface potential of CBECC-TENGs with (a) 2.0% CB contents and (b) without CB; Surface charge density of CBECC-TENGs with (c) 2.0% CB contents and (d) without CB.

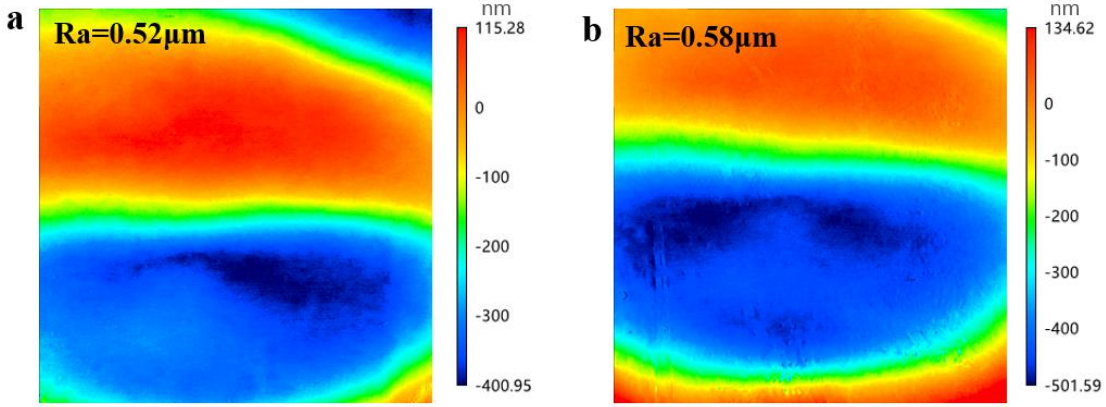


Figure S4. PDMS morphology diagrams (a) before and (b) after 5000 cycles of testing.

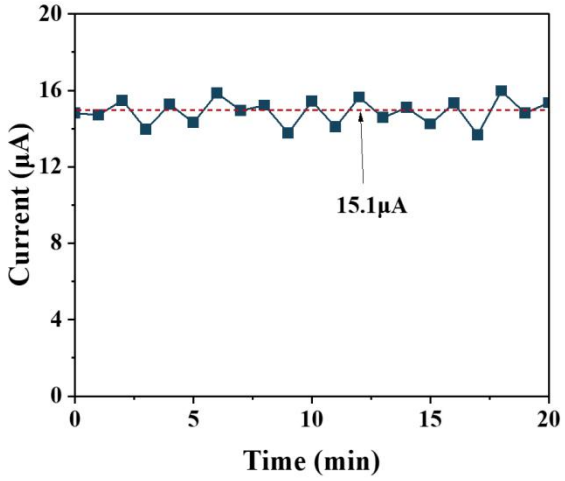


Figure S5. The output current of the rectified CBECC-TENGs for cathodic protection.